

# Numerical studies for localization–delocalization transition in vibrational spectra

B.J. Huang, Ten-Ming Wu\*

*Institute of Physics, National Chiao-Tung University, HsinChu 300, Taiwan*

## ARTICLE INFO

### Article history:

Received 27 February 2010  
 Received in revised form 25 June 2010  
 Accepted 12 July 2010  
 Available online 16 July 2010

### Keywords:

Localization–delocalization transition  
 Level-spacing statistics  
 Multifractal analysis  
 Instantaneous normal modes

## ABSTRACT

By investigating the localization–delocalization transition (LDT) in the instantaneous-normal-mode spectrum of a simple fluid, we compare two numerical methods, the level-spacing statistics and the multifractal analysis, for determining the LDT in vibrational spectra. Both methods are based on scale invariance at the transition. Within numerical errors, our results of the two methods give a reasonable agreement on the location of the transition.

© 2010 Elsevier B.V. All rights reserved.

## 1. Introduction

Disorder-induced localization–delocalization transition (LDT), also known as Anderson transition, has been an interesting topic for over fifty years [1]. For infinite systems at the LDT, the correlation length  $\xi_\infty$  diverges with a power law with a critical exponent  $\nu$ , indicating that there is no relevant length scale at the transition. For finite systems of linear size  $L$ , as the cases in numerical calculations, the LDT is usually referred to the one-parameter scaling theory [2], in which a macroscopic variable is a unique scaling function of the ratio  $L/\xi_\infty$ . The exponent  $\nu$  is universal and characterized by the universality class of the disordered systems. Meanwhile, strong fluctuations of the eigenfunctions at the LDT exhibit a multifractal nature, due to the self-similarity of the system on all length scales [3].

The location of LDT by spectral methods is usually determined by two numerical methods: the level-spacing (LS) statistics and the multifractal analysis (MA), commonly based on the scale invariance of a system at the LDT. In the LS statistics, the correlations between the discrete levels at an LDT is independent of the system size  $L$  [4]. In the MA, the multifractality at an LDT is described by the singularity spectrum  $f(\alpha)$ , which is a set of the fractal dimensions for the points with the eigenfunction intensity scaled as  $L^{-\alpha}$ . Generally,  $f(\alpha)$  is a convex function with a maximum at  $\alpha_0$  equal to the space dimension of the system. Another feature point in  $f(\alpha)$  is the one where  $f(\alpha_1) = \alpha_1$ , so that the slope of  $f(\alpha)$  at  $\alpha_1$  is one. The scale invariance of  $f(\alpha)$  at an LDT suggests that the constancy of the singularity strength  $\alpha_0$  and  $\alpha_1$  with  $L$  serves the conditions for determining the location of the LDT [5].

Recently, we have investigated the LDT in the instantaneous-normal-mode (INM) spectrum of a truncated Lennard-Jones (TLJ) fluid, which is a prototype of topologically disordered systems [6]. Generalized from the phonon concept in solid-state physics for describing the short-time dynamics of fluids, the INMs are referred as the eigenmodes of the Hessian matrices evaluated at fluid configurations [7]. By the LS statistics and the finite-size scaling, two LDTs, one with a positive eigenvalue and the other with a negative eigenvalue, are found in the INM spectrum. Within numerical errors, the estimated critical exponents of the two LDTs agree with each other and are close to that of the Anderson model in three dimensions. On the other hand, the LDT in the vibrational spectrum of fcc lattices with force-constant disorder has been studied with the MA [8]. Also, with the advance in computers and algorithms for calculating the Anderson model (AM) in large scales, the accuracy for the singularity spectrum of the AM has been much improved [9–11]. In this paper, using the two numerical approaches, we further investigate the location of the negative-eigenvalue LDT in the INM spectrum of the TLJ fluid and the obtained results are compared.

## 2. Level-spacing statistics

The thermodynamic state of the TLJ fluid is chosen at reduced density  $\rho^* = 0.972$  and reduced temperature  $T^* = 0.836$  [12]. With the periodic boundary conditions for  $N$  particles confined in a cube of length  $L$ , the fluid configurations are generated by Monte Carlo simulation, and  $N$  is varied from 3000 to 96000. The Hessian matrices of the TLJ fluid are diagonalized with Lanczos algorithm [13]. Presented in Ref. [6], the normalized INM spectrum consists of two branches, corresponding to the positive and negative eigenvalues. With the LS statistics given below for  $N$  less than 3000, the

\* Corresponding author.

E-mail address: [tmw@faculty.nctu.edu.tw](mailto:tmw@faculty.nctu.edu.tw) (T.-M. Wu).

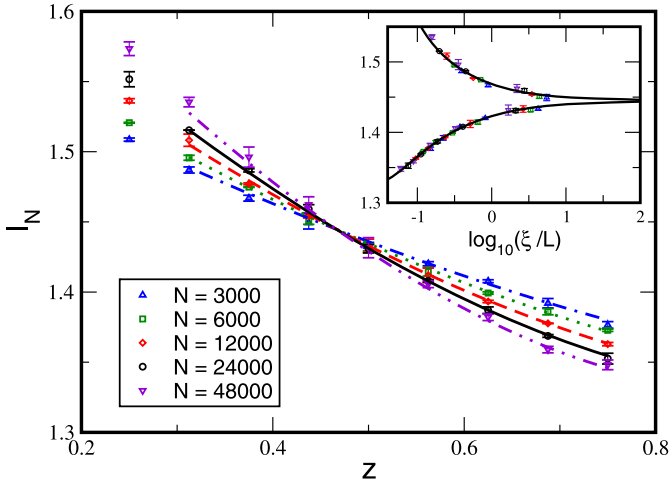


**Fig. 1.** The second moment  $I_N$  of  $P(s)$  for INMs near the LDT in the negative-eigenvalue branch.  $N$  is the particle number in simulation. The symbols are obtained by the numerical eigenvalues. The lines are the fit results of model  $(n, m) = (3, 1)$  for  $z$  within  $[0.3125, 0.75]$ . The inset shows the scaling function of  $I_N(z)$ .

LDT in the negative-eigenvalue branch is found to occur between  $-95$  and  $-80$ .

For each system size, the INM eigenvalues  $\lambda$  from  $-95$  to  $-80$  are unfolded to make the density of states of the unfolded eigenvalues  $z$  uniform. Then, these unfolded eigenvalues are further divided into small sections. For each section, the second moment  $I_N$  of the nearest-neighbor LS distribution  $P(s)$  is calculated; the data as a function of  $z$  are presented in Fig. 1 for five system sizes. For each  $N$ ,  $I_N$  monotonically increases from the delocalized to the localized region in the INM spectrum. Generally, due to the size dependence of  $P(s)$ ,  $I_N$  increases with  $N$  in the localized region but decreases in the delocalized region. The scale invariance of  $P(s)$  at the LDT indicates that  $I_N$  is independent of  $N$  at some  $z_c$ , which is the location of the LDT.

Since the crossing points of the  $I_N$  curves in Fig. 1 do not shift systematically with  $N$ ,  $I_N(z)$  generally follows the one-parameter scaling theory and can be described by a function  $f(\chi(Z)L^{1/\nu})$ , where the relevant scaling variable  $\chi(Z)$  is a function of  $Z = (z_c - z)/z_c$  that measures the deviation from the transition point. The nonlinearity of the  $I_N$  curves in Fig. 1 implies that  $f(x)$  and  $\chi(Z)$  should be nonlinear functions of their variables [14]. We approximate  $f(x)$  and  $\chi(Z)$  with the Taylor series up to order  $n$  and  $m$ , respectively.

$$f(\chi(Z)L^{1/\nu}) = \sum_{i=0}^n a_i \chi(Z)^i L^{i/\nu}, \quad \chi(Z) = \sum_{j=1}^m b_j Z^j, \quad (1)$$

where  $b_1 = 1$ . Each model with the approximated  $f(x)$  and  $\chi(Z)$  is specified with  $(n, m)$ , and the fitting parameters of the model include all expansion coefficients,  $z_c$  and  $\nu$ .

With the models  $(n, m) = (2, 2)$ ,  $(3, 1)$ ,  $(2, 3)$  and  $(3, 2)$ , which numbers of fitting parameters are less than eight, we fit the  $I_N$  data within a region of  $z$  chosen differently. An accepted fit is determined by two criterions: the goodness  $Q$  of the fit is larger than 0.01 [14] and the error bar of  $\nu$  is less than 0.2. Shown in Fig. 1, the best fit, with  $Q = 0.092$ , is the one with  $(n, m) = (3, 1)$  for  $z$  within  $[0.3125, 0.75]$ . The best fit gives  $\nu = 1.57 \pm 0.04$ , which is consistent with that of the AM [15], and the location of the LDT at  $\lambda_c = -86.96 \pm 0.05$ . After the system sizes are scaled by the correlation length  $\xi(z) = C|\chi(Z)|^{-\nu}$ , where  $C$  is a constant, the  $I_N$  data of the five system sizes indeed collapse onto a single scaling function.

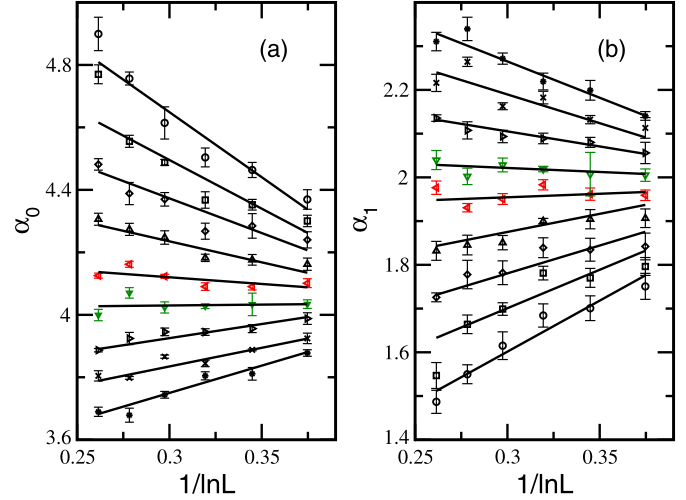


**Fig. 2.** Scaling of  $\alpha_0$  (a) and  $\alpha_1$  (b) with  $(\ln L)^{-1}$ . Indicated with different symbols, the data from top to bottom for  $\alpha_0$  and in reversed order for  $\alpha_1$  are averaged for INMs within eigenvalue intervals centered from  $-91.1$  to  $-83.1$  and with  $\Delta\lambda = 1$ . The symbols close to the LDT have different colors. The lines are the linear fit for the data of each interval.

### 3. Multifractal analysis

In MA, the eigenvectors of INMs are needed. For a configuration of  $N$  particles, there are  $3N$  INM eigenvectors, corresponding to discrete eigenvalues  $\lambda_s$  ( $s = 1, \dots, 3N$ ). Generated with the JADAMILU package [16], the  $3N$  components of a normalized INM eigenvector are denoted as  $\mathbf{e}_j^s$  for  $j = 1, \dots, N$ , where  $\mathbf{e}_j^s$  is the three-dimensional projection vector of particle  $j$  in the INM [17]. Following the box-counting procedure [3], we divide the simulation box of size  $L$  into  $N_\eta = \eta^{-3}$  smaller boxes of size  $l$ , with  $\eta = l/L$ . The measure for the squared vibrational amplitudes of INM  $s$  in the  $k$ -th small box is given as

$$\mu_k^s(\eta) = \sum_{j \in \text{box } k} |\mathbf{e}_j^s|^2. \quad (2)$$

The singularity strength  $\alpha_q$  is, therefore, defined as

$$\alpha_q = \lim_{\eta \rightarrow 0} \frac{1}{\ln \eta} \left\langle \sum_{k=1}^{N_\eta} \frac{(\mu_k^s(\eta))^q}{P_q^s(\eta)} \ln \mu_k^s(\eta) \right\rangle, \quad (3)$$

where  $P_q^s(\eta)$  is a summation of  $(\mu_k^s(\eta))^q$  over all small boxes and  $\langle \dots \rangle$  denotes an arithmetic average over the INMs with  $\lambda_s$  within an interval of width  $\Delta\lambda$  centered at  $\lambda$ . It is impossible to take the limit in Eq. (3) for the finite-size systems. Alternatively, the  $\alpha_q$  value can be obtained by the slope of a linear fit for the average value in Eq. (3) versus  $\ln \eta$ . In our calculations,  $\eta$  is set between 0.1 and 0.5 for each  $L$ .

Fig. 2 shows  $\alpha_q$ , with  $q = 0, 1$ , versus the inverse of  $\ln L$  for  $N$  from 3000 to 96000, with each data point obtained by averaging  $1.5 \times 10^3$  INMs within an interval of  $\Delta\lambda = 1$ . By taking for granted the  $\lambda_c$  value from the LS statistics, the center of the eigenvalue interval is chosen from  $-83.1$  to  $-91.1$ . Following Ref. [8], we define  $g_i = d\alpha_i/d(\ln L)^{-1}$  as the slope of the linear-fit function in Fig. 2 for each eigenvalue interval. The constancy of  $\alpha_i$  with  $L$  gives the  $\lambda_c$  value. Indicated by the zero-value of  $g_i$  in Fig. 3,  $\lambda_c$  is estimated near  $-86.6$ , with an error equal to one.

### 4. Conclusions

In summary, using the LS statistics and the MA, we have investigated numerically the LDT in the negative-eigenvalue INM

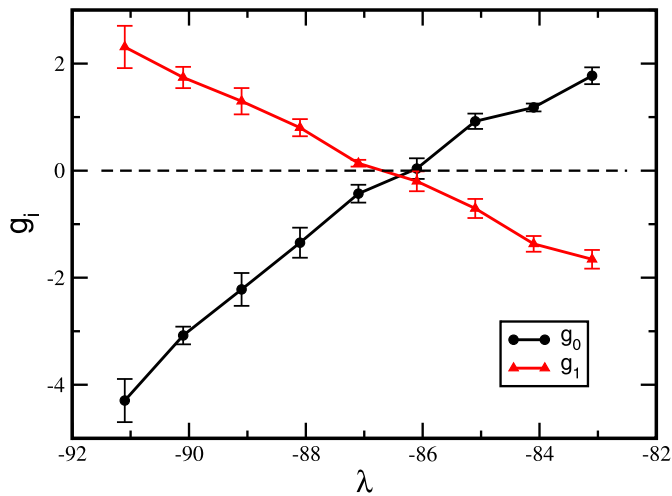


**Fig. 3.** Variation of  $g_i$  with  $\lambda$ . The circles and triangles, with the lines to guide the eye, are for  $g_0$  and  $g_1$ , respectively. The zero-crossing point of the  $g_i$  line predicts  $\lambda_c = -86.6 \pm 0.5$ .

spectrum of a TLJ fluid. Scale invariance at the LDT is the fundamental theme of the two methods. Within numerical errors, the two methods give a reasonable agreement on the location of the

LDT. The LS statistics makes a profit on the critical exponent; the MA is economic in computer time.

### Acknowledgement

T.M. Wu acknowledge financial support from National Science Council of Taiwan under No. NSC 97-2112-M-009-0005-MY2.

### References

- [1] P.W. Anderson, Phys. Rev. 109 (1958) 1492.
- [2] E. Abrahams, P.W. Anderson, D.C. Licciardello, T.V. Ramakrishnan, Phys. Rev. Lett. 42 (1979) 673.
- [3] M. Schreiber, H. Grussbach, Phys. Rev. Lett. 67 (1991) 607.
- [4] B.I. Shklovskii, B. Shapiro, B.R. Sears, P. Lambrianides, H.B. Shore, Phys. Rev. B 47 (1993) 11487.
- [5] F. Milde, R.A. Römer, M. Schreiber, Phys. Rev. B 55 (1997) 9463.
- [6] B.J. Huang, T.M. Wu, Phys. Rev. E 79 (2009) 041105.
- [7] R.M. Stratt, Acc. Chem. Res. 28 (1995) 201.
- [8] J.J. Ludlam, S.N. Taraskin, S.R. Elliott, Phys. Rev. B 67 (2003) 132203.
- [9] L.J. Vazquez, A. Rodriguez, R.A. Römer, Phys. Rev. B 78 (2008) 195106.
- [10] A. Rodriguez, L.J. Vazquez, R.A. Römer, Phys. Rev. B 78 (2008) 195107.
- [11] A. Rodriguez, L.J. Vazquez, R.A. Römer, Phys. Rev. Lett. 102 (2009) 106406.
- [12] T.M. Wu, W.J. Ma, S.F. Tsay, Physica A 254 (1998) 257.
- [13] J.K. Cullum, R.A. Willoughby, Lanczos Algorithms for Large Symmetric Eigenvalue Computations, Birkhäuser, Boston, 1985.
- [14] F. Milde, R.A. Römer, M. Schreiber, Phys. Rev. B 61 (2000) 6028.
- [15] K. Slevin, T. Ohtsuki, Phys. Rev. Lett. 82 (1999) 382.
- [16] M. Bollhöfer, Y. Notay, Comput. Phys. Comm. 177 (2007) 951.
- [17] T.M. Wu, W.J. Ma, J. Chem. Phys. 110 (1999) 447.